Safe UAV landing: A low-complexity pipeline for surface conditions recognition

Konstantinos A. Tsintotas, Loukas Bampis, Anastasios Taitzoglou, Ioannis Kansizoglou, and Antonios Gasteratos

2021 IEEE International Conference on Imaging Systems and Techniques (IST) | 978-1-7281-7371-9/21/$31.00 ©2021 IEEE | DOI: 10.1109/IST50367.2021.9651358

***Abstract*— As an unmanned aerial vehicle (UAV) navigates autonomously, there are unanticipated occasions, e.g., loss of data provided by the global navigation satellite system, where its mission has to be terminated. In such circumstances, the platform needs to change its navigation mode to landing, so as to protect the system from a possible accident. This process demands the successful selection of the ground surface before the aircraft starts its landing. This paper proposes a low-complexity algorithm for recognizing the suitability of the ground surface based on three laser range-finders, which are mounted on a hybrid vertical take-off and landing (VTOL) fixed-wing UAV. We take advantage of their small size, high precision distance measurements, and operational speed to compute the ground slope and the existence of any obstacles therein. Experiments on a prototype aircraft show that our method can perform robustly and under real-time constraints.**

I. Introduction

In robotic literature, multi-copter platforms are also known as micro aerial vehicles (MAVs) or unmanned aerial vehicles (UAVs). In recent years, these systems have become widely popular in the research community due to the market's demands for various military, commercial, and industrial applications [1], while their great progress is mainly owed to the technology's advances [2], [3]. Representative examples include traffic and farming surveillance [4], [5], asset monitoring [6], [7], wildfire detection [8], hazardous environments' investigation [9], [10], [11], product delivery [12], [13], structure inspection (such as power cables, dam walls, vessels, and bridges) [14], [15], [16], and search and rescue missions [17], [18], [19], [20].

The system's take-off, trajectory tracking, and precise landing constitute the main three components for achieving such autonomous tasks. However, among the objectives mentioned above, which are primarily based on a global positioning system (GPS) [21], autonomous landing is the most challenging part. This is because the flight controller has to generate a proper trajectory while minimizing power consumption and provide robustness in the face of dynamic conditions, e.g., sudden wind gusts or rotor downwash [22], moving landing platform [23], or unsuitable landing surfaces, e.g., rocky surroundings or high slope planes [24]. Moreover, methods based on GPS are susceptible to interference [25], which increases the accident rate when landing is performed in complex environments. Based on the above, frameworks leveraging the UAV's safe landing have become a popular research topic. Nevertheless, most techniques try to address the problem of detecting a landing platform [26], ignoring the surface condition, which can be proven disastrous for the vehicle's integrity.

Over the past decade, a significant amount of research on tracking and landing via visual navigation has been carried out [27], [28]. Using a vision-based system in different vehicle types [29], [30], [31], [32], including vertical take-off and landing (VTOL) platforms [33], [34], is a reliable solution due to its low cost [35] and low-interference characteristics [36], [37], [38], [39]. Besides, as most image-based computer vision algorithms for recognizing surface conditions [40], [41], [42] are prone to errors, researchers may turn their attention towards robust measurements from laser scanners [43], [44], such as light detection and ranging (LIDAR) [45], [46], as sources of information to perform a precise landing.

Since this process holds a vital role in the mission's integrity when developing a fully autonomous UAV, in this paper, we are interested in using a lightweight and low-complexity perception system, based on three range-finder sensors, for evaluating the surface's adequacy for landing. The original inspiration for our work comes from [24], where the authors used ultrasonic sensors employed in each copter's arm to measure the distance between the platform and the ground and avoided unsuitable surfaces by adopting heuristic techniques. However, the proposed system is designed to recognize the surface's slope together with potential obstacles therein and perform safety landing while still maintaining its complexity under real-time constraints. Our experiments were carried out on a prototype hybrid VTOL fixed-wing UAV [47], [48], dubbed as MPU RX-4. The main contributions proposed by the paper at hand are summarized as follows:

- A straightforward pipeline for recognizing increased slope surface during the landing process. This way, the risk of collision between the platform's parts and the ground is avoided while the system's integrity is ensured.
- A low-complexity algorithm for detecting protruding objects, e.g., rocks or tree trunks, in cases of a smooth ground slope.

The structure of the paper is as follows. Section II provides a problem definition. Section III describes the proposed methodology in detail, while its performance is evaluated in Section IV. The conclusion and future work are discussed in the last Section V.

Authors are with the Department of Production and Management Engineering, Democritus University of Thrace, 12 Vas. Sophias, GR-671 32, Xanthi, Greece {ktsintot, lbampis, ataitzog, ikansizo, agaster}@pme.duth.gr

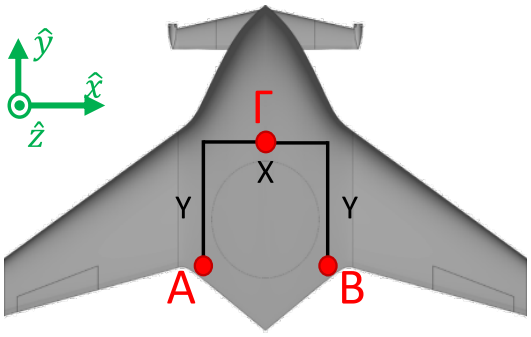

Fig. 1: An overview of the sensors' position in the proposed vertical take-off and landing (VTOL) aircraft. Points A and B, at the back of the aircraft, denote the two low-range laser ranger-finders. The third one, Γ, is the long-range distance sensor located at the center of the unmanned aerial vehicle.

II. Problem Statement

The task refers to recognizing the surface's conditions, which would permit the aircraft to land safely. MPU RX-4 is capable of vertical landing on its underbelly by utilizing a set of 3 propellers, while different sensors, e.g., global navigation satellite system (GNSS) receiver, accelerometer, range-finders, and inertial measurement unit (IMU), are mounted on its platform. However, for its autonomous landing, only the laser range-finders and the IMU are considered. The three laser sensors are facing down and are employed for measuring its altitude above the ground. More specifically, one long-range range-finder is used both for landing and navigation, while the rest are low-range ones and are utilized solely for landing.

III. Autonomous Landing

When the communication between the UAV and the ground station is interrupted, or the system needs to stop its operation due to an urgent situation in its working environment, autonomous landing should be chosen. Firstly, the vehicle descends slowly, using the long-range laser range-finder until it reaches a ground distance of 5 meters. Then, the other two sensors are activated, and the surface evaluation process begins. In order to measure the landing area's conditions, i.e., computing the surface's slope and any objects therein, the proposed perception framework uses the range-finders' output to calculate the dominant surface's plane. Based on this computation, its slope is estimated, and the vehicle is prompt to move elsewhere if the terrain is unsuitably steep or anomalous. Moreover, by exploiting the aircraft's continuous hovering and using a sequence of consecutive measurements, it can detect and avoid objects affecting the landing process. If the recognized landing ground conditions are satisfied, the aircraft continues its descending and sensing procedures until touching down.

A. Perception

For calculating a plane, three distance measurements between the UAV and the candidate landing ground are required. These figures can be used as distinct points since the sensor's location upon the aircraft's body is known. In Fig. 1, the proposed arrangement of the flight system's range-finders is presented. The low-range sensors are located at the back of the aircraft while the long-range to its center.

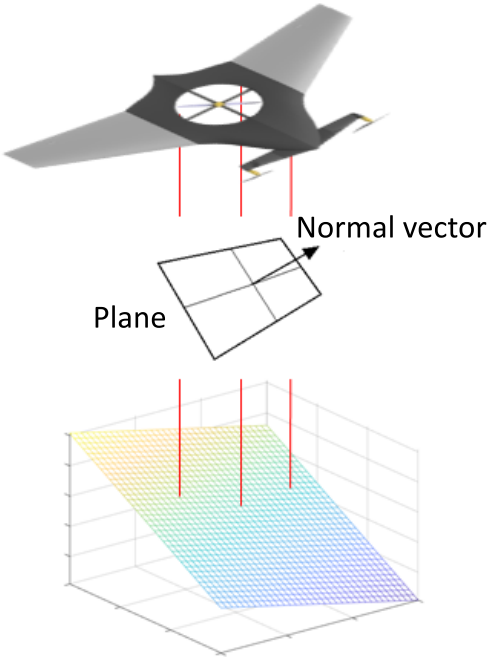

Fig. 2: The process of autonomous landing. When the aircraft reaches an altitude of 5 meters, its low-range distance sensors are activated. The data given by these range-finders and the measurement provided by the long-range sensor are used for the plane computation and, subsequently, its slope identification.

B. Surface slope estimation

Considering that the lengths X and Y (see Fig. 1) are known from the system's design and that Z_{A}, Z_{B}, and Z_{Γ} are the corresponding sensors' distance measurements, the points needed for the plane's computation are defined with respect to the UAV's frame of reference as:

$$P_A = \begin{bmatrix} 0 \\ 0 \\ Z_{\mathrm{A}} \end{bmatrix}, P_B = \begin{bmatrix} \mathrm{X} \\ 0 \\ Z_{\mathrm{B}} \end{bmatrix}, P_{\Gamma} = \begin{bmatrix} \mathrm{X}/2 \\ \mathrm{Y} \\ Z_{\Gamma} \end{bmatrix}. \quad (1)$$

By converting the measurements provided by the IMU into a rotation matrix R and assuming no horizontal translation for the vehicle[1], these points are expressed in the world's frame of reference as follows:

$$P'_A = RP_A, P'_B = RP_B, P'_{\Gamma} = RP_{\Gamma}. \quad (2)$$

Employing these data into the general plane equation:

$$ax + by + cz + d = 0 \quad (3)$$

[1]In case of horizontal translations, the respective information can be retrieved by the vehicle's pose estimation module and GNSS measurements.

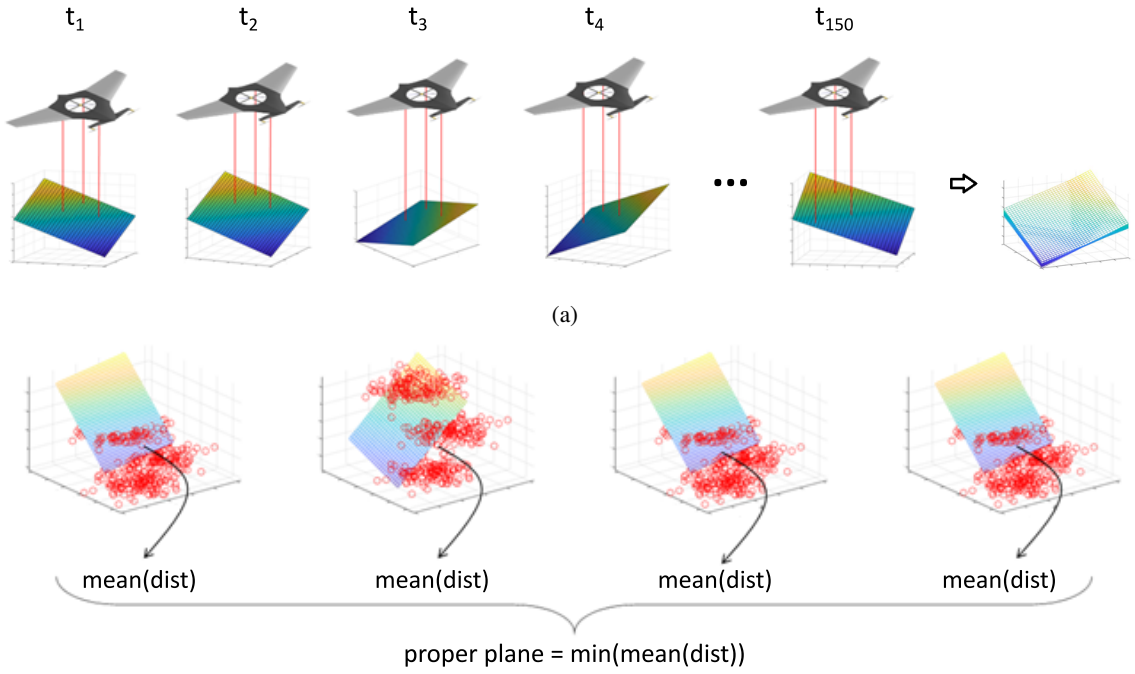

Fig. 3: Different distance measurements captured by the unmanned aerial vehicle's range-finders for consecutive time instances yield to the corresponding planes' calculation (a). Then, each plane is evaluated against the total of points recorded, and the one presenting the lowest average distance is selected as the dominant plane (b). Outlier points that are located beyond this plane, are used to identify potentially dangerous protruding objects on the surface.

each parameter a, b, c is calculated. Note that the last parameter d is set to 0 since it does not affect the plane's slope, just its displacement. The vector $N = [a, b, c]^T$ constitutes the normal vector of the plane, whose angles with respect to the horizontal plane are calculated through:

$$\cos(\phi) = \frac{N \cdot N_0}{|N||N_0|}, \tag{4}$$

where $N_0 = [0, 0, -1]^T$ refers to the normal vector of the horizontal plane. The proposed methodology is summarized in the representative example depicted in Fig. 2.

C. Robust surface and protruding object detection

During the UAV's landing process, the distance measurements taken at each time step from the laser sensors correspond to several points. Hence, a point cloud of the surface is generated wherein different planes can be computed, as shown in Fig 3a. We choose to exploit the hovering movement, which occurs as the aircraft descends to the ground, to compute the existence of any object in the candidate landing place using a scheme based on random sample consensus (RANSAC) [49]. Keeping a total of 150 consecutive instances, the average distance between the recorded points and each plane is computed. The plane Q with the lowest score is chosen as dominant one (see Fig. 3b). Outlying points which are located beyond Q can be used to identify protruding objects that may harm the platform's integrity during landing.

(a) (b) (c)

Fig. 4: The landing area where our experiments took place. Our unmanned aerial vehicle (UAV) was tested on three scenarios, viz., flat (a), increased slope (b), and rocky (c). Experiments took place in an outdoor environment within our university's campus.

IV. Experimental protocol

This section presents the experiments that took place in a static environment for evaluating the landing algorithm's performance. The control commands were sent wirelessly to the aircraft, while the proposed algorithm was responsible for allowing or preventing the system's landing. Experiments carried out in an outdoor area of our university campus using three different cases of surface, viz., flat, increased slope, and rocky (see Fig. 4).

TABLE I: MPU RX-4 specifications.

	Specifications
Type	Vertical take-off and landing (VTOL)
Dimensions (W × H)	1800mm × 1000mm
Maximum take-off weight	7.5 Kg
Flight Time	60 minutes (with fully take-off weight)
Flight controller	Hex Cube Black (known as Pixhawk 2.1)
Onboard computer	Intel Edison
Laser range-finder (1)	TeraRanger One (up to 14 meters)
Laser range-finder (2)	TeraRanger One (up to 14 meters)
Laser range-finder (3)	LightWare SF11/C (up to 120 meters)

A. Experimental platform

The used hybrid VTOL fixed-wing UAV is a custom-made platform constructed and assembled from scratch. Table I displays its overall specifications. More specifically, it is equipped with a Hex Cube Black[2] flight controller (previously known as Pixhawk 2.1) flashed with PX4[3] software. This autopilot suite constitutes a commercially available software providing internal access to its flight controller and its parameters. The landing algorithm is executed on an Intel Edison processor mounted internally to the controller as a companion computer, aiming to increase the system's computational capabilities. The corresponding custom software was built on the Linux operating system hosted by the companion computer. Data are provided by the sensor to the controller and subsequently to the companion computer via the Inter-Integrated Circuit (I^2C) and micro aerial vehicles communication protocol (MAVLink[4]). This way, the Hex Cube Black is utilized as an off-the-shelf solution for reading the acquired distance measurements. Concerning the down-facing laser modules, an SF11/C[5] has been installed as the long-range (120 meters) distance sensor, while two TeraRanger One[6] are employed as low-range (14 meters) ones. In Fig. 5, the proposed flight system is presented, while the prototype UAV equipped with the mentioned sensors is shown in Fig. 6.

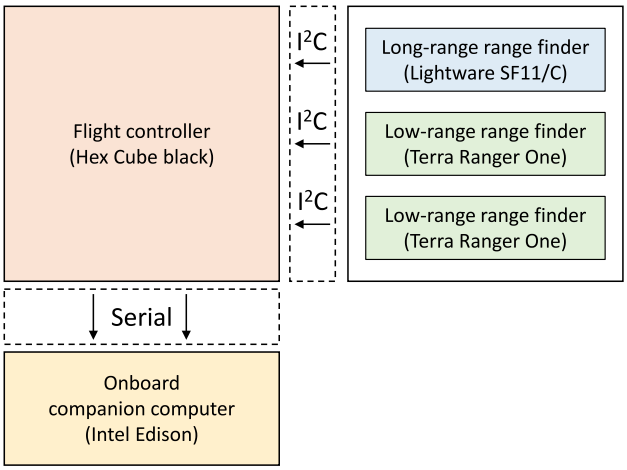

Fig. 5: An overview of the proposed landing system. In conjunction with the flight controller's inertial measurement unit (IMU) data, measurements recorded from the three range-finders are processed by the companion computer, which is embedded on the platform for computing the ground surface conditions.

Fig. 6: The unmanned aerial vehicle used for our experiments. It includes a Hex Cube Black flight controller incorporating an Intel Edison companion computer. Three laser range-finders (one SF11/C and two Terra Ranger One) are employed for the system's perception during the landing procedure.

B. Results

Our platform was tested in two different scenarios. The first regards a terrain which is suitable for landing. We assessed our algorithm on a flat surface without obstacles or significant slope. Nevertheless, for the second scenario, two extra cases were evaluated. More specifically, the first was a surface that presented an increased slope ($>30^o$), whereas the second was a surface with a stone.

1) Suitable for landing: By hovering the aircraft over a metallic slab within a low grass landing area (see Fig. 4a), we performed four trials in different environmental conditions, i.e., day-time and afternoon, as well as sunny and cloudy. During each landing trial, our hybrid VTOL fixed-wing UAV was able to recognize that the surface conditions were suitable for performing its landing procedure. Distance measurements acquired from the laser range-finders have shown a slight deviation due to the grass; however, the system achieved to detect the plane's slope with high accuracy, due to the proposed RANSAC-based scheme.

2) Not suitable for landing: A set of trials was held in a similar manner for testing the detection algorithm when the aircraft encounters an unsuitable ground surface. Regarding the case of an increased slope, a surface with at 40^o was selected. The system was able to compute the ground's slope with $\pm 5^o$ accuracy during each trial. Concerning the last test case, the landing area presented a large stone therein (Fig.

[2]https://tinyurl.com/HexCubeBlack
[3]https://tinyurl.com/px4io
[4]https://tinyurl.com/mavlinkio
[5]https://tinyurl.com/sf11-c-120m
[6]https://tinyurl.com/teraranger1

TABLE II: Average processing time needed for recognizing the surface conditions.

		Time (ms)
Sensor data	Long-range range-finder	9.2
	Low-range range-finder (1)	6.5
	Low-range range-finder (2)	6.6
Plane computation	Points' rotation	20.2
	Plane computation	40.8
Landing place recognition	Slope computation	10.9
	Robust surface detection	55.8
Whole algorithm		150.0

4c). During each evaluation trial, the system detected that the ground's slope was not flat canceling its landing process due to the stone's size.

C. System's complexity

Given that for safe navigation, real-time constraints must be satisfied, one of the most crucial requirements of the proposed algorithm regards its execution time. In order to completely showcase the complexity of the landing process, we evaluated each part of our method individually. In Table II, an extensive assessment of the corresponding response times is presented. It is worth noting that our system computes the surface conditions at 6.66 Hz, which sufficiently satisfies the real-time constraints by detecting hazardous situations faster than the platform's locomotion to its next descending position.

V. Conclusions and future work

In this paper, we designed a perception system for protecting the integrity of a UAV's platform in cases of emergency landings. The proposed framework follows a low complexity pipeline able to be adapted to small and light aircrafts. Using the distance measurements provided by three laser range-finders mounted on the UAV's underbelly, our system evaluates the surface conditions by computing the plane on which the UAV attempts to land. This way, we achieve to verify the suitability of the landing area through the computation of the plane's slope. At the same time, any obstacle included on the respective area is detected to avoid collisions. Our evaluation protocol have been based on three cases, namely flat, increased slope, and rocky, revealing the efficiency of the proposed method. In the future, we plan to build a geofenced system for protecting the autonomous UAV both during landing and navigation, while more experiments are intended to be held for testing our method's robustness.

VI. Acknowledgment

This work has been implemented within the project "MPU-Multirole Portable UAS" which has been financially supported by the European Regional Development Fund, Partnership Agreement for the Development Framework (2014-2020), co-funded by Greece and European Union in the framework of OPERATIONAL PROGRAMME: "Competitiveness, Entrepreneurship and Innovation 2014-2020 (EPAnEK)", Nationwide Action: "Research - Create - Innovate" (project code: T1EDK-00737).

References

[1] B. Canis, "Unmanned aircraft systems (UAS): Commercial outlook for a new industry." Congressional Research Service Washington, DC, 2015.

[2] K. P. Valavanis, *Advances in unmanned aerial vehicles: state of the art and the road to autonomy*. Springer Science & Business Media, 2008.

[3] K. P. Valavanis and G. J. Vachtsevanos, *Handbook of unmanned aerial vehicles*, vol. 1. Springer, 2015.

[4] M. A. Khan, W. Ectors, T. Bellemans, D. Janssens, and G. Wets, "UAV-based traffic analysis: A universal guiding framework based on literature survey," *Transp. Research Procedia*, vol. 22, pp. 541–550, 2017.

[5] D. Reiser, D. Paraforos, M. Khan, H. Griepentrog, and M. Vázquez-Arellano, "Autonomous field navigation, data acquisition and node location in wireless sensor networks," *Precision Agriculture*, vol. 18, no. 3, pp. 279–292, 2017.

[6] S. S. Congress, A. J. Puppala, and C. L. Lundberg, "Total system error analysis of UAV-CRP technology for monitoring transportation infrastructure assets," *Engineering Geology*, vol. 247, pp. 104–116, 2018.

[7] S. M. Adams and C. J. Friedland, "A survey of unmanned aerial vehicle (UAV) usage for imagery collection in disaster research and management," in *Proc. Int. Workshop on Remote Sensing for Disaster Response*, vol. 8, 2011.

[8] T. Giitsidis, E. G. Karakasis, A. Gasteratos, and G. C. Sirakoulis, "Human and fire detection from high altitude uav images," in *Proc. Euromicro Int. Conf. on Parallel, Distributed, and Network-based Processing*, (Turku, Finland), pp. 309–315, Mar. 2015.

[9] E. Lygouras, I. M. Dokas, K. Andritsos, K. Tarchanidis, and A. Gasteratos, "Identifying hazardous emerging behaviors in search and rescue missions with drones: A proposed methodology," in *Proc. Int. Conf. Information Systems for Crisis Response and Management in Mediterranean Countries*, (Xanthi, Greece), pp. 70–76, Oct. 2017.

[10] R. S. De Moraes and E. P. De Freitas, "Multi-UAV based crowd monitoring system," *IEEE Trans. Aerospace and Electronic Systems*, vol. 56, no. 2, pp. 1332–1345, 2019.

[11] R. Y. Brogaard, O. Ravn, and E. Boukas, "Absolute localisation in confined spaces using deep geometric features," *Electronics Letters*, 2021.

[12] B. D. Song, K. Park, and J. Kim, "Persistent UAV delivery logistics: MILP formulation and efficient heuristic," *Computers & Industrial Engineering*, vol. 120, pp. 418–428, 2018.

[13] I. T. Papapetros, V. Balaska, and A. Gasteratos, "Multi-layer map: Augmenting semantic visual memory," in *Proc. Int. Conf. Unmanned Aircraft Systems*, (Athens, Greece), pp. 1206–1212, Sep. 2020.

[14] R. Fan, J. Jiao, J. Pan, H. Huang, S. Shen, and M. Liu, "Real-time dense stereo embedded in a UAV for road inspection," in *Proc. IEEE/CVF Conf. Computer Vision and Pattern Recognition Workshops*, (Long Beach, CA, USA), pp. 0–0, Jun. 2019.

[15] M. Banić, A. Miltenović, M. Pavlović, and I. Ćirić, "Intelligent machine vision based railway infrastructure inspection and monitoring using UAV," *Facta Universitatis, Series: Mechanical Engineering*, vol. 17, no. 3, pp. 357–364, 2019.

[16] R. Andersen, L. Nalpantidis, O. Ravn, and E. Boukas, "Investigating Deep Learning Architectures towards Autonomous Inspection for Marine Classification," in *Proc. IEEE International Symposium on Safety, Security, and Rescue Robotics*, pp. 197–204, 2020.

[17] A. Amanatiadis, E. G. Karakasis, L. Bampis, T. Giitsidis, P. Panagiotou, G. C. Sirakoulis, A. Gasteratos, P. Tsalides, A. Goulas, and K. Yakinthos, "The HCUAV project: Electronics and software development for medium altitude remote sensing," in *Proc. IEEE Int. Symp. on Safety, Security, and Rescue Robotics*, pp. 1–5, 2014.

[18] E. Lygouras, A. Gasteratos, K. Tarchanidis, and A. Mitropoulos, "ROLFER: A fully autonomous aerial rescue support system," *Microprocessors and Microsystems*, vol. 61, pp. 32–42, 2018.

[19] E. Lygouras, N. Santavas, A. Taitzoglou, K. Tarchanidis, A. Mitropoulos, and A. Gasteratos, "Unsupervised human detection with an embedded vision system on a fully autonomous UAV for search and rescue operations," *Sensors*, vol. 19, no. 16, p. 3542, 2019.

[20] V. A. Feraru, R. E. Andersen, and E. Boukas, "Towards an Autonomous UAV-based System to Assist Search and Rescue Operations in Man Overboard Incidents," in *Proc. IEEE International Symposium on Safety, Security, and Rescue Robotics*, pp. 57–64, 2020.

[21] J. Farrell and M. Barth, *The global positioning system and inertial navigation*, vol. 61. Mcgraw-hill New York, NY, USA, 1999.

[22] M. Veismann, C. Dougherty, and M. Gharib, "Experimental studies of the rotor flow downwash on the stability of multi-rotor crafts in descent," in *APS Division of Fluid Dynamics Meeting Abstracts*, (Denver, Colorado), pp. M18–002, Nov. 2017.

[23] B. Herissé, T. Hamel, R. Mahony, and F.-X. Russotto, "Landing a VTOL unmanned aerial vehicle on a moving platform using optical flow," *IEEE Trans. Robotics*, vol. 28, no. 1, pp. 77–89, 2011.

[24] M. Hamanaka and F. Nakano, "Surface-condition detection system of drone-landing space using ultrasonic waves and deep learning," in *Proc. Int. Conf. Unmanned Aircraft Systems*, (Athens, Greece), pp. 1452–1459, Sep. 2020.

[25] C.-S. Yoo and I.-K. Ahn, "Low cost GPS/INS sensor fusion system for UAV navigation," in *Proc. Digital Avionics Systems Conference*, vol. 2, (Indianapolis, IN, USA), pp. 8–A, Oct. 2003.

[26] T. Baca, P. Stepan, and M. Saska, "Autonomous landing on a moving car with unmanned aerial vehicle," in *Proc. Eur. Conf. Mobile Robots*, (Paris, France), pp. 1–6, Sep. 2017.

[27] M. B. Vankadari, K. Das, C. Shinde, and S. Kumar, "A reinforcement learning approach for autonomous control and landing of a quadrotor," in *Proc. Int. Conf. Unmanned Aircraft Systems*, (Dallas, TX, USA), pp. 676–683, Jun 2018.

[28] J. S. Wynn and T. W. McLain, "Visual servoing for multirotor precision landing in daylight and after-dark conditions," in *Proc. Int. Conf. Unmanned Aircraft Systems*, (Atlanta, GA, USA), pp. 1242–1248, Jun. 2019.

[29] S. Lange, N. Sunderhauf, and P. Protzel, "A vision based onboard approach for landing and position control of an autonomous multirotor UAV in GPS-denied environments," in *Proc. Int. Conf. Advanced Robotics*, (Munich, Germany), pp. 1–6, Jun. 2009.

[30] N. Kyriakoulis and A. Gasteratos, "Color-based monocular visuoinertial 3-D pose estimation of a volant robot," *IEEE Trans. Instrumentation and Measurement*, vol. 59, no. 10, pp. 2706–2715, 2010.

[31] K. A. Tsintotas, L. Bampis, and A. Gasteratos, "DOSeqSLAM: Dynamic on-line sequence based loop closure detection algorithm for SLAM," in *Proc. IEEE Int. Conf. Imaging Systems and Techniques*, (Krakow, Poland), pp. 1–6, IEEE, Oct. 2018.

[32] K. A. Tsintotas, P. Giannis, L. Bampis, and A. Gasteratos, "Appearance-based loop closure detection with scale-restrictive visual features," in *Proc. Int. Conf. Computer Vision Systems*, (Thessaloniki, Greece), pp. 75–87, Sep. 2019.

[33] S. Saripalli, J. F. Montgomery, and G. S. Sukhatme, "Visually guided landing of an unmanned aerial vehicle," *IEEE Trans. Robotics and Automation*, vol. 19, no. 3, pp. 371–380, 2003.

[34] X. Yang, H. Pota, M. Garratt, and V. Ugrinovskii, "Prediction of vertical motions for landing operations of uavs," in *Proc. IEEE Conf. Decision and Control*, (Cancun, Mexico), pp. 5048–5053, Dec. 2008.

[35] Y. Bi and H. Duan, "Implementation of autonomous visual tracking and landing for a low-cost quadrotor," *Optik-International Journal for Light and Electron Optics*, vol. 124, no. 18, pp. 3296–3300, 2013.

[36] K. A. Tsintotas, L. Bampis, and A. Gasteratos, "Probabilistic appearance-based place recognition through bag of tracked words," *IEEE Robotics and Automation Letters*, vol. 4, no. 2, pp. 1737–1744, 2019.

[37] R. Fan, J. Jiao, H. Ye, Y. Yu, I. Pitas, and M. Liu, "Key ingredients of self-driving cars," in *Proc. Eur. Sig. Processing Conference Satellite Workshop on Signal Processing, Computer Vision and Deep Learning for Autonomous Systems*, (A Coruna, Spain), Sep. 2019.

[38] K. A. Tsintotas, L. Bampis, and A. Gasteratos, "Tracking-DOSeqSLAM: A dynamic sequence-based visual place recognition paradigm," *IET Computer Vision*, vol. 15, no. 4, pp. 258–273, 2021.

[39] K. A. Tsintotas, L. Bampis, and A. Gasteratos, "Modest-vocabulary loop-closure detection with incremental bag of tracked words," *Robotics and Autonomous Systems*, vol. 141, p. 103782, 2021.

[40] W. Kong, D. Zhou, D. Zhang, and J. Zhang, "Vision-based autonomous landing system for unmanned aerial vehicle: A survey," in *Proc. Int. Conf. Multisensor Fusion and Information Integration for Intelligent Systems*, (Beijing, China), pp. 1–8, Sep. 2014.

[41] E. Boukas and A. Gasteratos, "Modeling regions of interest on orbital and rover imagery for planetary exploration missions," *Cybernetics and Systems*, vol. 47, no. 3, pp. 180–205, 2016.

[42] Y. Wang, W. Wen, S. Wu, C. Wang, Z. Yu, X. Guo, and C. Zhao, "Maize plant phenotyping: comparing 3D laser scanning, multi-view stereo reconstruction, and 3D digitizing estimates," *Remote Sensing*, vol. 11, no. 1, p. 63, 2019.

[43] J. A. Bellian, C. Kerans, and D. C. Jennette, "Digital outcrop models: applications of terrestrial scanning lidar technology in stratigraphic modeling," *J. Sedimentary Research*, vol. 75, no. 2, pp. 166–176, 2005.

[44] M. A. Balduzzi, D. Van der Zande, J. Stuckens, W. W. Verstraeten, and P. Coppin, "The properties of terrestrial laser system intensity for measuring leaf geometries: a case study with conference pear trees," *Sensors*, vol. 11, no. 2, pp. 1657–1681, 2011.

[45] D. Burton, D. B. Dunlap, L. J. Wood, and P. P. Flaig, "Lidar intensity as a remote sensor of rock properties," *J. Sedimentary Research*, vol. 81, no. 5, pp. 339–347, 2011.

[46] A. F. Errington, B. L. Daku, and A. F. Prugger, "Reflectance modelling using terrestrial lidar intensity data," in *Proc. IEEE Int. Conf. Imaging Systems and Techniques*, (Macau, China), pp. 1–6, Sep. 2015.

[47] P. E. Kaparos, C. D. Bliamis, and K. Yakinthos, "Conceptual design of a UAV with VTOL characteristics," in *AIAA Aviation Forum*, (Dallas, Texas, USA), p. 3137, Jun. 2019.

[48] C. Bliamis, I. Zacharakis, P. Kaparos, and K. Yakinthos, "Aerodynamic and stability analysis of a VTOL flying wing UAV," in *IOP Conf. Series: Materials Science and Engineering*, (Suzhou, China), p. 012039, Jan. 2021.

[49] F. Mufti, R. Mahony, and J. Heinzmann, "Robust estimation of planar surfaces using spatio-temporal RANSAC for applications in autonomous vehicle navigation," *Robotics and Autonomous Systems*, vol. 60, no. 1, pp. 16–28, 2012.